Consequences of cAMP-Binding Site Mutations on the Structural Stability of the Type I Regulatory Subunit of cAMP-Dependent Protein Kinase[†]

Jaume M. Cànaves,[‡] Darryl A. Leon,[‡,§] and Susan S. Taylor*

Department of Chemistry and Biochemistry, 0654, University of California, San Diego, 9500 Gilman Drive, La Jolla, California 92093-0654

Received July 6, 2000; Revised Manuscript Received October 5, 2000

ABSTRACT: The regulatory (R) subunit of cAMP-dependent protein kinase (cAPK) is a multidomain protein with two tandem cAMP-binding domains, A and B. The importance of cAMP binding on the stability of the R subunit was probed by intrinsic fluorescence and circular dichroism (CD) in the presence and absence of urea. Several mutants were characterized. The site-specific mutants R(R209K) and R(R333K) had defects in cAMP-binding sites A and B, respectively. R(M329W) had an additional tryptophan in domain B. Δ(260−379)R lacked Trp260 and domain B. The most destabilizing mutation was R209K. Both CD and fluorescence experiments carried out in the presence of urea showed a decrease in cooperativity of the unfolding, which also occurred at lower urea concentrations. Unlike native R, R(R209K) was not stabilized by excess cAMP. Additionally, CD revealed significant alterations in the secondary structure of the R209K mutant. Therefore, Arg209 is important not only as a contact site for cAMP binding but also for the intrinsic structural stability of the full-length protein. Introducing the comparable mutation into domain B, R333K, had a smaller effect on the integrity and stability of domain A. Unfolding was still cooperative; the protein was stabilized by excess cAMP, but the unfolding curve was biphasic. The R(M329W) mutant behaved functionally like the native protein. The Δ(260−379)R deletion mutant was not significantly different from wild-type RIα in its stability. Consequently, domain B and the interaction between Trp260 and cAMP bound to site A are not critical requirements for the structural stability of the cAPK regulatory subunit.

The major receptor for cAMP in eukaryotic cells, cAMP-dependent protein kinase (cAPK),[1] is present in all mammalian tissues and regulates a wide variety of metabolic processes. In the absence of cAMP, cAPK exists as an inactive tetramer consisting of a dimeric regulatory (R) subunit and two catalytic (C) subunits. Binding of cAMP to the R subunits causes the tetrameric complex to dissociate into an R dimer and two free C subunits (*1*). In addition to its role as an inhibitor of the C subunit, the R subunit anchors the holoenzyme to specific intracellular sites (*2*) and it prevents the C subunit from entering the nucleus (*3*).

Although several forms of the R subunit are expressed, all have a conserved and well-defined domain structure (*1*) (Figure 1, cartoon). Each region not only has its own function but also communicates with other regions as part of the conformational changes that are induced by the binding of cAMP. This domain structure, characterized originally by limited proteolysis, was subsequently confirmed using recombinant techniques (*4*). The N-terminus is a requirement for dimerization (*5*−*9*) and for anchoring or docking at specific subcellular locations (*9*−*12*). Next, there is a short region that inhibits the catalytic subunit, and finally, there are two tandem and homologous cAMP-binding domains at the C-terminus, designated as A and B (*13*, *14*) (Figure 1, cartoon). These two cAMP-binding domains, presumably resulting from gene duplication, show extensive sequence similarity and bind cAMP cooperatively (*15*, *16*). A model for each cAMP-binding domain was proposed on the basis of the crystal structure of the homologous catabolite gene activator protein (CAP) from *Escherichia coli* (*17*), and subsequently, the crystal structure of the Δ(1−91)R deletion mutant was determined (*18*) (Figure 1A).

The RIα subunit contains three tryptophans (*13*) (Figure 1, cartoon and panel A) that can be used to monitor unfolding (*19*, *20*). Two of these, Trp188 and Trp222, are located in cAMP-binding domain A. The third, Trp260, lies at the junction between domains A and B, and its aromatic side chain stacks with the adenine ring of the cAMP bound to site A (*18*) (Figure 1B).

[†] This work was supported in part by U.S. Public Health Service Grant GM34921 to S.S.T. D.A.L. was supported in part by a Minority Supplement grant (GM34921), a Department of Education Graduate Assistance in Areas of National Need (GAANN) Fellowship, and U.S. Public Health Service Training Grant GM07313-16.

* To whom correspondence should be addressed. E-mail: staylor@ucsd.edu. Fax: (858) 543-8193.

[‡] These authors contributed equally to this work and should both be considered first authors.

[§] Present address: DoubleTwist, Inc., 1999 Harrison St., Suite 1100. Oakland, CA 94612.

[1] Abbreviations: cAPK, cAMP-dependent protein kinase; C, catalytic; R, regulatory; wt-R, wild-type RIα regulatory; MOPS, 3-(*N*-morpholino)propanesulfonic acid; EDTA, ethylenediaminetetraacetic acid; cAMP, adenosine 3′,5′-cyclic monophosphate; SDS−PAGE, sodium dodecyl sulfate−polyacrylamide gel electrophoresis; CD, circular dichroism; Θ_{222}, mean residue ellipticity at 222 nm; C_m, midpoint concentration at which 50% of the protein is unfolded; λ_{max}, wavelength of maximum fluorescence emission; Trp, tryptophan.

10.1021/bi001563q CCC: $19.00
Published on Web 11/14/2000

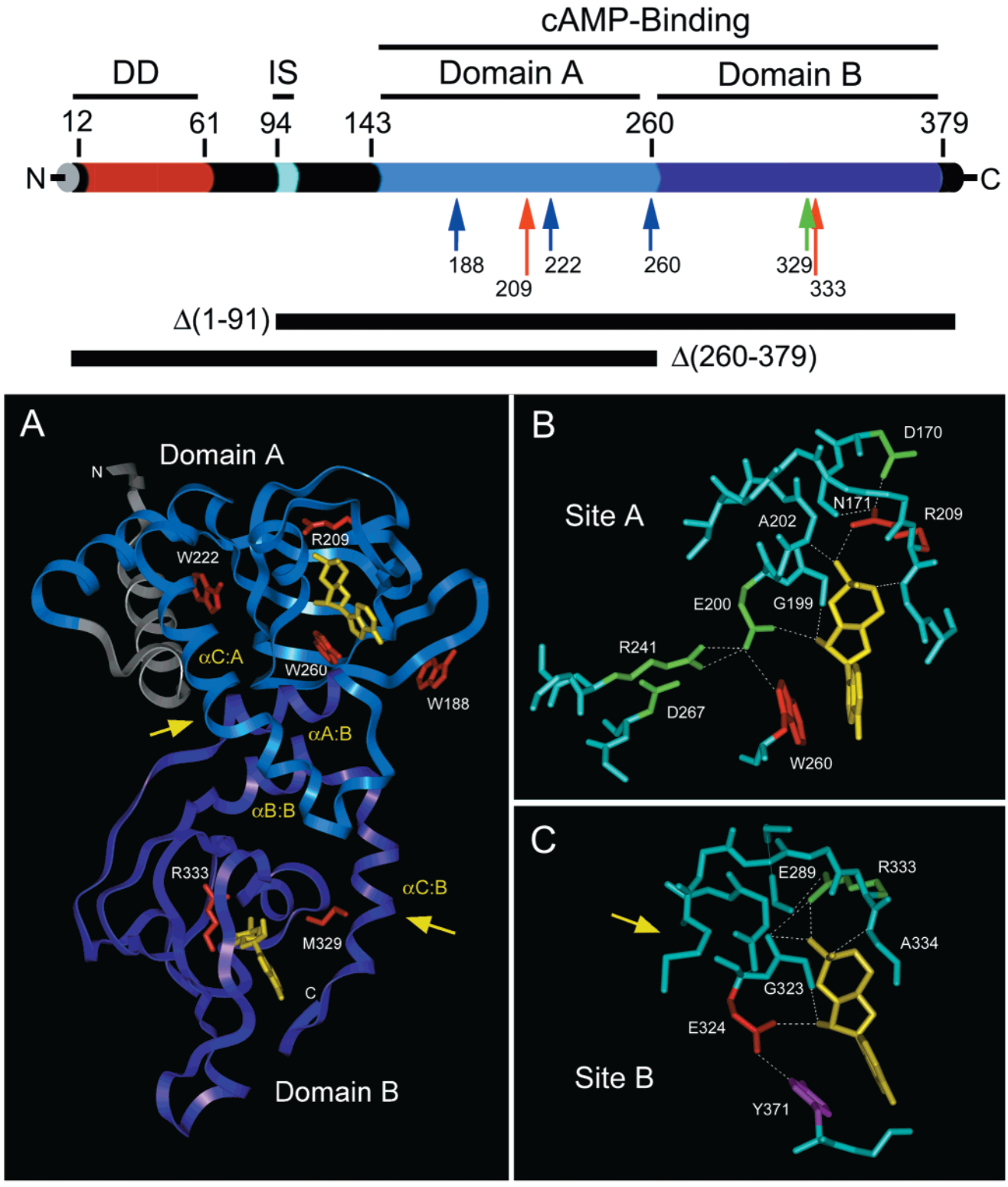

FIGURE 1: Schematic diagram and summary of the domain structure and mutants of the type I regulatory subunit of the cAMP-dependent protein kinase. (Cartoon) Location of the N-terminal dimerization domain (red), autoinhibitory region (cyan), cAMP-binding domain A and B (blue and purple, respectively), and intrinsic tryptophans (blue arrows). Red arrows indicate residues that interact directly with cAMP and have been mutated. In R(M329W), an additional Trp residue has been introduced (green arrow). Bars in the lower part of the cartoon indicate the relative lengths of the Δ(1−91)R deletion mutant used to elicit the crystal structure of RIα, and the domain B-defective Δ(260−379)R mutant. (A) Ribbon representation of the general architecture of Δ(1−91) RIα. The N-terminal region is gray; domain A is blue, and domain B is purple. Both cAMP molecules are yellow. The side chains of intrinsic Trp residues, Arg residues that interact with cAMP, and the Met residue replaced with Trp in R(M329W) are red. Yellow arrows indicate α-helices C:A and C:B. (B and C) Views of the hydrogen-bonding interactions between cAMP and the protein in domains A and B, respectively. Possible H-bonds are represented by dashed lines (distances of <3.3 Å). The yellow arrow indicates position 329, where a new Trp residue is introduced in R(M329W).

One of the most important challenges related to cAPK is to understand the conformational changes that are associated with forming and breaking the holoenzyme complex. A complex network of interactions links the two cAMP-binding domains in R. In the holoenzyme, site A is masked so that cAMP binds initially to site B and induces a conformational change that makes site A accessible to cAMP (*21*, *22*). cAMP binding to site A then promotes dissociation of C. This is a highly cooperative process in which domain B serves as a "gate" to regulate access of cAMP to domain A. Peripheral interaction sites required for high-affinity binding to C are also localized near the A domain (*23*, *24*).

Although the general ligand binding properties of the two cAMP-binding sites have been well characterized, less is known about the conformational changes associated with the binding process as well as the determinants of the structural stability of each domain. Also, the dynamics of interdomain communication and the transference of conformational changes to the inhibitor site to trigger holoenzyme dissociation need to be investigated in more detail.

In the work presented here, we have explored how altering the cAMP-binding properties of each cAMP-binding domain influences the global structural integrity of the cAPK regulatory subunit, and how changes in one domain can influence the neighboring domain.

EXPERIMENTAL PROCEDURES

Mutagenesis. The oligonucleotide-directed *in vitro* Mutagenesis System kit (Bio-Rad) was used to replace a Met codon with a Trp codon at position 329 in pLST1, a pUC118-based vector that contained the RIα gene (*25*), as described previously (*19*, *26*). The oligonucleotide primer was synthesized on an Applied Biosystems DNA Synthesizer. The resulting mutant clones were identified by DNA sequencing of randomly picked plaques following transformation of *E. coli* JMIO1. DNA sequencing was carried out according to the dideoxy method (*27*) using Sequenase (United States Biochemical). The mutant RI genes were expressed in *E. coli* 222 according to the method of Saraswat et al. (*26*). RIα mutants R(R209K) (*28*), R(R333K) (*29*), and Δ(260−279)R (*4*, *30*) were constructed and expressed as described previously.

Protein Preparation. The wild-type RIα subunit (wt-R) and mutant proteins were purified by anion exchange chromatography (*19*) or by affinity chromatography using cAMP−agarose resin (T. Diller et al., unpublished results). For the second process, cell homogenates were subjected to two ammonium sulfate precipitation steps. The pellet resulting from a first precipitation with 30% ammonium sulfate was discarded, and the ammonium sulfate concentration in the supernatant was increased to 60%. The pellet resulting from this second precipitation was resuspended, incubated overnight with the cAMP resin, and eluted with an excess of cAMP at room temperature. Purified proteins were concentrated using Centricon-10 concentrators and stored in 50% glycerol at −80 °C. The protein purity was confirmed by SDS−PAGE in 12.5% acrylamide gels. The expression of the mutant proteins was comparable to that of the native protein.

To remove the tightly bound cAMP from the R subunits, purified proteins were incubated with 8 M urea in 5 mM MOPS, 0.5 mM EDTA, l00 mM KCl, and 5 mM β-mercaptoethanol (pH 7.0) (buffer A) for 3 h. A Pharmacia NAP-10 column prepacked with Sephadex G-25 and equilibrated with 8 M urea in buffer A was used to separate the protein from the cAMP. After the peak fractions containing the R subunit had been pooled, urea was removed by dialysis against buffer A (*31*). Since the R subunits are more labile to proteolysis when cAMP is not bound, or when they are not part of a holoenzyme complex (*12*), experiments were performed within 2 days of stripping.

Urea Denaturation of the R Subunits. Stock solutions of 8 M urea and 150 mM cAMP were prepared in buffer A and/or buffer B (buffer A without KCl) for the fluorescence experiments, and in buffer C (buffer A without KCl or β-mercaptoethanol) for the CD experiments. The 8 M urea solutions were used within 1 week of preparation. The 3 M KI, 3 M NaCl, and 10 mM sodium thiosulfate used in iodide quenching measurements were prepared in buffer B. All the solutions were made with reagent-grade or higher-grade chemicals and filtered prior to use. Proteins (0.5−1.0 μM) were unfolded in various concentrations of urea for 3 h at room temperature. Overnight incubation produced no additional changes in the fluorescence emission.

Circular Dichroism Data Acquisition and Analysis. Proteins (0.1 mg/mL) were in buffer C. CD measurements were performed on an AVIV 202 CD spectropolarimeter using a 0.1 cm path length microcuvette (40 μL capacity). All buffers and stock solutions were filtered through a 0.2 μm cellulose acetate filter. CD spectra were scanned at 25 °C from 260 to 190 nm, at a 1 nm resolution and with an integration time of 10 s. Each measurement was performed in triplicate. Deviations between scans were negligible. Baseline subtraction was performed using the AVIV CDS program. Conversion of observed ellipticities (millidegrees) to mean residue ellipticities (degrees per square centimeter per decimole) was calculated for each point in the spectra according to the equation

$$\mathrm{MRE}_\lambda = \Theta_\lambda M_{\mathrm{avg}}/(10LC)$$

where Θ_λ is the measured ellipticity in millidegrees at wavelength λ, M_{avg} is the average mass per amino acid, 10 is a scaling factor, L is the path length of the sample cell in centimeters, and C is the concentration of the protein in milligrams per milliliter. Fast Fourier transform filter smoothing of the curves was performed using the Microcal Origin version 3.5 program. CD spectra were deconvoluted using the CDNN program version 2.0.3 (*32*) and a NNET_33 trained neural network. Additional deconvolutions were performed using the self-consistent method (*33*), the variable-selection method (*34*, *35*) included in the Dichoprot program (*36*), and the neural network-based K2D program (*37*).

Fluorescence Data Acquisition and Analysis. Fluorescence measurements were carried out in 1 cm quartz cuvettes at 23 °C using a Hitachi F4010 fluorometer. Samples were excited at 293 nm, and tryptophan emission was monitored from 300 to 450 nm. Fractional unfolding curves were calculated by using the relationship

$$F_{\mathrm{U}} = 1 - [(R - R_{\mathrm{U}})/(R_{\mathrm{F}} - R_{\mathrm{U}})]$$

where F_{U} is the fraction of unfolded protein, R is the observed

ratio of intensity at 353 nm to 340 nm at various urea concentrations, and R_F and R_U represent the values of R for the folded and unfolded states, respectively. The transition regions of the denaturation curves were used to describe the thermodynamics of the unfolding by assuming a simple two-state model. In a two-state mechanism, $F_N + F_U = 1$, where F_N and F_U are the fractions of native and unfolded protein, respectively.

The ΔG for the unfolded protein at zero concentration of denaturant, $\Delta G_U^{H_2O}$, was calculated according to the linear extrapolation method using the equation $\Delta G_U = \Delta G_U^{H_2O} - m$[urea], where the slope m is a parameter that indicates the degree of cooperativity of the unfolding process and ΔG_U is the free energy of denaturation at each urea concentration (*38*). ΔG_U values were calculated from the fraction of folded and unfolded protein according to the following relationships: $F_N/F_U = K_U$, $K_U = e^{-\Delta G_U/R.T}$, and $-RT \ln(F_U/F_N) = \Delta G_U$.

Potassium iodide (KI) quenching measurements were carried out on samples containing R subunits (0.5 μM), KI (0−0.3 M), and selected urea concentrations (0, 3, and ∼7 M). KI was dissolved in buffer B. Since I_3^- absorbs in the region of tryptophan fluorescence, a small amount of sodium thiosulfate (0.1 mM) was added to the KI solution. The ionic strength ($\mu = 0.3$) was kept constant with NaCl. Quenching data were plotted using the Stern−Volmer equation [$F_o/F = 1 + K$[X], where F_o/F is the fractional decrease in fluorescence due to a quencher X and K is the Stern−Volmer quenching constant (*39*)]. The fraction of tryptophan fluorescence quenched was estimated by plotting the fluorescence quenching data against the quencher concentration using the modified Stern−Volmer equation:

$$F_o/\Delta F = 1/f_a K[Q] + 1/f_a$$

where F_o is the fluorescence in the absence of quencher, ΔF is F_o minus the fluorescence observed in the presence of a quencher, f_a is the fraction of accessible tryptophans, K is the Stern−Volmer constant of quenching, and [Q] is the molar concentration of quencher (*40*).

RESULTS

With the exception of R(M329W), the purification and physical properties of the rest of the mutants, i.e., R(R209K) (*41*), R(R333K) (*29*), and Δ(260−379)R (*4*, *30*), have been described previously. The two proteins with point mutations in the cAMP-binding sites, R(R209K) and R(R333K), have an approximately 10-fold lower affinity for cAMP (*29*, *42*), whereas Δ(260−379)R binds cAMP with high affinity and forms tight complexes with the C subunit (*43*). R(M329W) was newly engineered to introduce a Trp residue in the vicinity of cAMP-binding site B (Figure 1C) to monitor the unfolding of domain B. In every functional aspect, R(M329W) was indistinguishable from wt-R. It bound cAMP with high affinity and formed a holoenzyme that could be activated with cAMP with a $K_{a(cAMP)}$ similar to that of the wild-type holoenzyme (data not shown). All full-length mutant R subunits migrated on SDS−PAGE gels with an apparent M_r that was indistinguishable from that of wt-R (47 kDa). Δ-(260−379)R migrated with an apparent M_r of 38 kDa.

Evaluation of Changes in Secondary Structure by Circular Dichroism. The CD spectra of wt-R and the mutants are typical of α-helical proteins (*44*) with double minimums at 208 and 222 nm. The spectra of wt-R, R(R333K), and R(M329W) were very similar (Figure 2), indicating that the global secondary structure of wt-R was not significantly affected by the point mutations. The CD spectrum of R(R209K) exhibited substantial differences. The ellipticity at 222 nm (Θ_{222}) (Figure 2) was lower than in the rest of the mutants, suggesting a lower α-helical content.

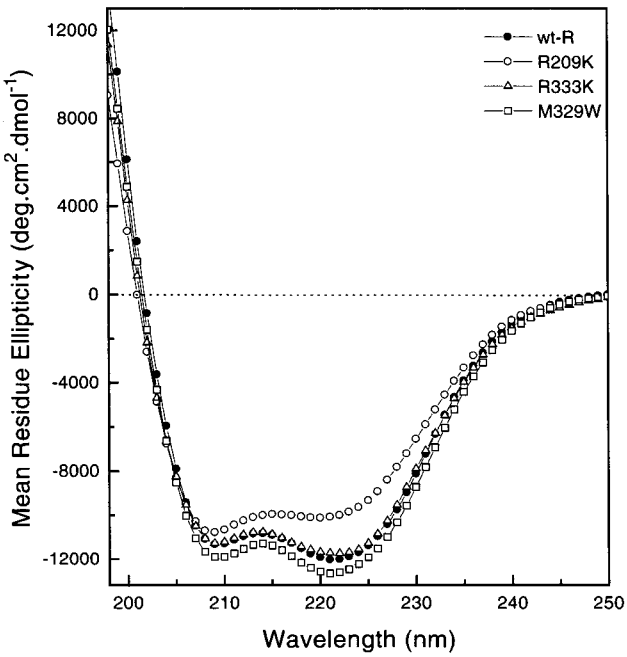

FIGURE 2: Far-UV CD spectra of wt-R and mutant proteins. The CD spectrum of each protein is designated as follows: wt-R (●), R(R209K) (○), R(R333K) (△), and R(M329W) (□). The protein concentration was 0.1 mg/mL. The CD spectrum was scanned from 260 to 190 nm at 25 °C in buffer C. The mean residue ellipticity is shown as a function of wavelength.

Several deconvolution methods (enumerated in Experimental Procedures) were evaluated. The CDNN method yielded the best correlation with empirical structural data. Deconvolution indicated a decrease (approximately 8%) in helicity in R(R209K) with respect to wt-R and the rest of the point mutants. No other statistically significant differences were observed between wt-R and the R(M329W) and R(R333K) mutants.

Fluorescence Emission Spectra of the Mutant Proteins. The fluorescence emission spectra of wt-R, R(M329W), and R(R333K) exhibited a λ_{max} of 340 nm in the absence of urea (Figure 3). In contrast, R(R209K) had a λ_{max} of 343 nm. The spectra of R(M329W) and R(R209K) exhibited a significant increase in the fluorescence intensity compared to that of wt-R. However, the most striking difference was the 39% increase in the intensity of the fluorescence emission for R(R209K). The increase in intensity for R(R209K) resembled what was observed when wt-R was stripped of cAMP (*19*), and suggested that R(R209K) did not have cAMP bound to domain A. We confirmed this by incubating R(R209K) with increasing concentrations of cAMP (Figure 4). As cAMP was added, the Trp fluorescence was quenched. The apparent dissociation constant appK_d(cAMP) was 1 μM, consistent with the previously determined appK_d for cAMP activation of the holoenzyme formed with R(R209K) (*42*). The emission spectrum for R(R333K) exhibited a reduction

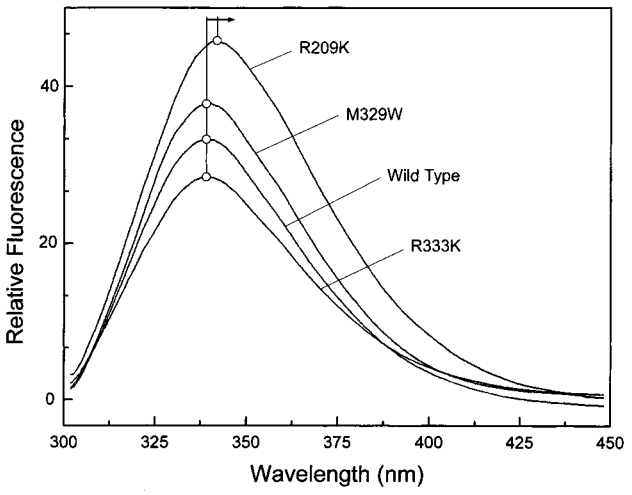

FIGURE 3: Comparison of the fluorescence emission spectra of wt-R and mutants. Samples (0.5 μM) containing wt-R, R(R209K), R(R333K), or R(M329W) were excited at 293 nm at 23 °C in buffer A. Each protein (0.5 μM R dimer) was saturated with cAMP. The arrow indicates the shift in λ_{max} for R(R209K) with respect to wt-R and the rest of the mutants.

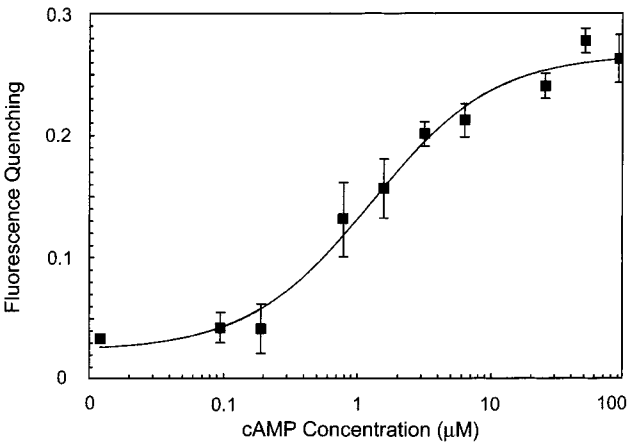

FIGURE 4: Quenching of the tryptophan fluorescence in the R(R209K) mutant by cAMP binding. The protein (0.5 μM) was dialyzed against buffer A before fluorescence measurements in the presence of increasing cAMP concentrations were performed.

of 15% in fluorescence intensity compared to that of wt-RI, indicating that the perturbation of cAMP-binding site B has long-range effects on the environment of the tryptophans in domain A. An increase of 15% in fluorescence was observed for R(M329W), which reflected the additional Trp in domain B.

Urea-Induced Unfolding Monitored by Intrinsic Fluorescence. The unfolding process between 0 and 4 M urea resulted in a 1.8 nm shift to red of the λ_{max} of wt-R. In contrast, the changes in λ_{max} for R(R209K) and R(R333K) were 7.6 and 3.3 nm, respectively (Figure 5B,D), indicating a substantial destabilizing effect by those two mutations. From 0 to 4 M urea, the changes in the emission of R(M329W) were comparable to those observed with wt-R (Figure 5A,C). The changes between 4 and 6 M urea, followed by the gradual increase in emission intensity at urea concentrations of >6 M, were also comparable. The global changes in the fluorescence intensity for R(M329W) were smaller than for wt-R.

The fractional unfolding curves and concentration midpoints (C_m) of wt-R and the mutants are compared in Figure 6 (white symbols) and Table 1. There were no significant differences between the profiles for wt-R and R(M329W) (Figure 6A,C). R(R209K) showed the most significant changes (Figure 6B). The unfolding curve for R(R209K) in the presence of increasing urea concentrations was shifted dramatically to lower concentrations. Whereas the C_m was 4.8 M for wt-R, it was 3.6 M for R(R209K), indicating that a substantial degree of structural destabilization resulted from the mutation. In fact, the C_m value for R(R209K) was even lower than the C_m for stripped wt-R [Figure 6A (×)]. Also, there was a decrease in the cooperativity of unfolding, as indicated by the lower *m* value. The decreases in cooperativity and free energy of unfolding were similar in magnitude to those observed for stripped wt-R (Table 1).

The unfolding profile for R(R333K) also shifted to lower urea concentrations (C_m = 4.3 M), resembling the change in C_m observed for stripped wt-R (C_m = 4.2 M). The *m* value was intermediate between those of the stripped wt-R and R(R209K), indicating the conservation of some cooperativity in the unfolding (Figure 6D). Additionally, the free energy of unfolding was intermediate between those of wt-R and R(R209K).

Urea-Induced Unfolding Monitored by CD. The stability of wt-R, R(M329W), R(R209K), and R(R333K) was monitored using far-UV CD in the presence of increasing concentrations of urea (Figure 7). The experimental conditions were identical to those used for the fluorescence experiments. Θ_{222} was used to monitor changes in secondary structure, since Θ_{222} is directly related to the α-helical content (*45*). Neither wt-R nor R(M329W) and R(R333K) showed any significant decrease in Θ_{222} at 4 M urea. In contrast, there was a 15% decrease in Θ_{222} at 4 M for R(R209K), indicating a substantial reduction in helicity relative to the other mutants and wt-R. At 5 M urea, there was a small decrease in Θ_{222} for wt-R. The reduction in Θ_{222} for R(M329W) and R(R333K) at 5 M was intermediate between wt-R and R(R209K). The largest change corresponded to R(R209K). At 6 M urea, the changes in Θ_{222} for wt-R, R(R333K), and R(M329W) were practically equivalent, and smaller than the reduction in Θ_{222} for R(R209K).

Effect of Excess cAMP on Stability. To examine whether excess cAMP stabilized the mutant R subunits in the transition region between 3 and 6 M urea, as it does for wt-R (*19*), unfolding was carried out in the presence of excess cAMP. The concentration of cAMP that was used (150 μM) is sufficient to saturate both wild-type and mutant cAMP-binding sites. Each of the three mutants (black symbols in Figure 6 and Table 1) behaved differently. The unfolding curve for R(R209K) (Figure 6B) showed no significant effect of excess cAMP on C_m. R(R333K) showed a unique unfolding curve in the presence of excess cAMP (Figure 6D). The C_m for R(R333K) in the absence of excess cAMP was only slightly lower than for wt-R. However, in the presence of excess cAMP, the unfolding curve for R(R333K) was not only shifted to higher urea concentrations as in wt-R but also biphasic. This suggested that under those conditions there was a stable intermediate. In the presence of excess cAMP, there were two components in the unfolding of R(R333K) (Figure 6D). The first had a C_m of 3.6 M, while the second had a C_m of 6.0 M, closely matching the C_m values for R(R209K) and wt-R, respectively. After the addition of 150 μM cAMP to R(M329W), the unfolding curve was

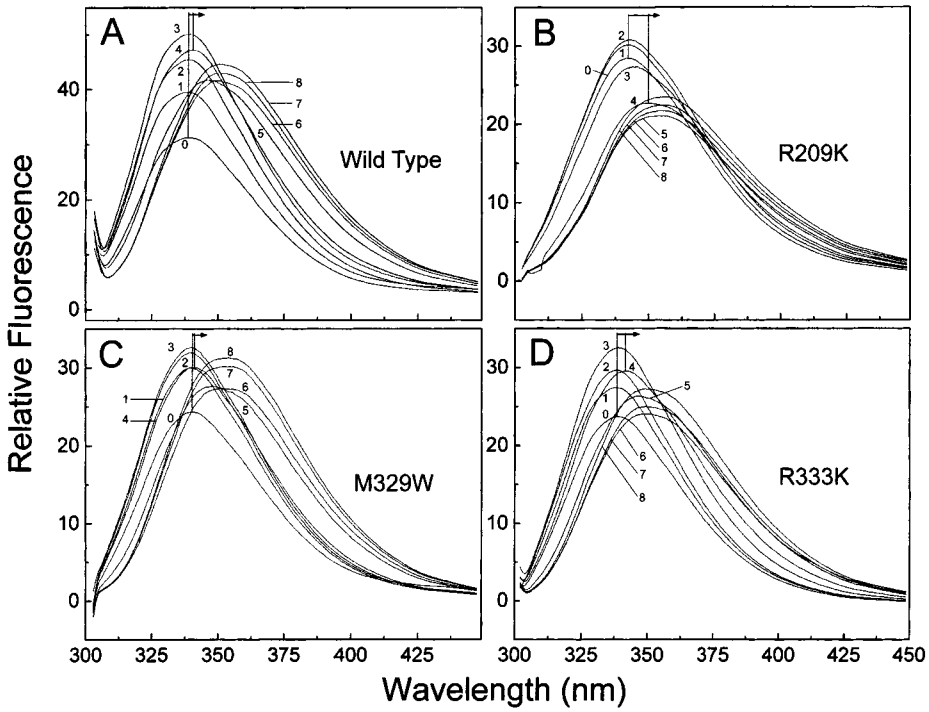

FIGURE 5: Tryptophan fluorescence spectra of wt-R and the R(R209K), R(R333K), and R(M329W) mutants at various urea concentrations. The urea concentrations are indicated on each spectrum. The protein samples (0.5 μM) were excited at 293 nm at 23 °C in buffer A. Arrows in each panel indicate the direction of the shift in λ_{max} due to the increase in urea concentration from 0 to 4 M.

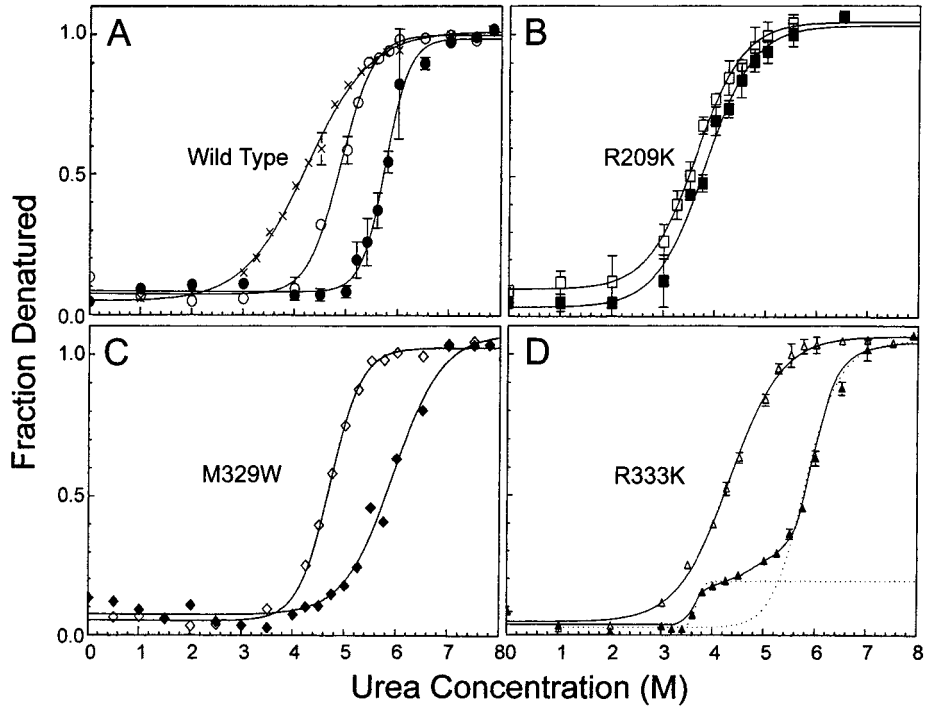

FIGURE 6: Unfolding curves for wt-R and the R(R209K), R(R333K), and R(M329W) mutants as a function of urea concentration. With the exception of the stripped R curve (×) in panel A, the data were taken from the fluorescence spectra in Figure 5. The R subunit dimer proteins (0.5 μM) were denatured in the absence of excess cAMP (white symbols) or in the presence of 150 μM excess cAMP (black symbols). wt-R and R(M329W) contain 4 mol of cAMP bound per mole of dimer, whereas R(R209K) and R(R333K) contain only 2 mol of cAMP bound per mole of dimer when purified. Dotted lines in panel D correspond to the deconvolution of the biphasic curve for R(R333K) in the presence of excess cAMP.

shifted to higher urea concentrations as in wt-R. Unlike wt-R, excess cAMP reduced the cooperativity of the unfolding of R(M329W).

Iodide Quenching. Fluorescence was monitored at 340 nm in the presence of 0 or 3 M urea, and at 353 nm in the presence of ~7 M urea. In the absence of urea, only 30% of the Trp fluorescence of wt-R was quenched. In contrast, R(R209K), R(R333K), and R(M329W) had 50, 50, and 40% of their Trp fluorescence quenched in the absence of denaturant, respectively. This indicated that the equivalent of one to two tryptophans could be quenched when no denaturant was present (Table 2). Quenching was larger for

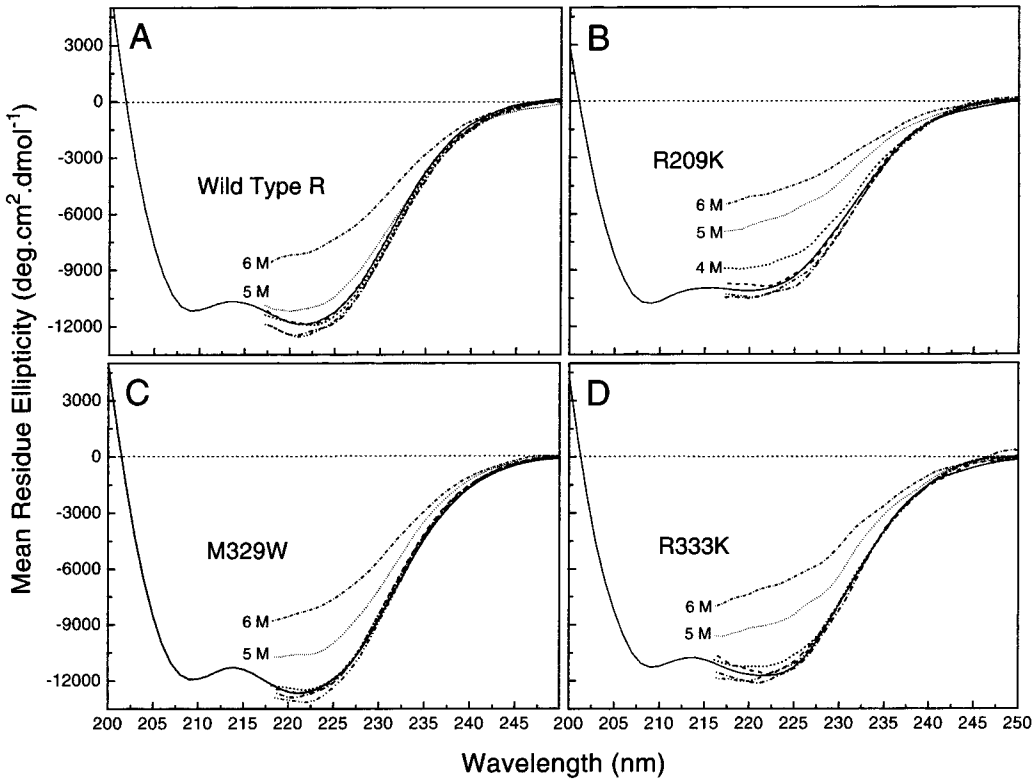

FIGURE 7: Urea denaturation of wt-R and the R(R209K), R(R333K), and R(M329W) mutants as monitored by far-UV CD. The CD spectra for each protein (0.1 mg/mL) were acquired in the presence of 0, 1, 2, 3, 4, 5, and 6 M urea in buffer C. The spectra were scanned from 260 to 190 nm at 25 °C. Spectra were filtered using a FFT filter. The mean residue ellipticity is shown as a function of wavelength.

Table 1: Midpoint Concentrations (C_m) of Wild-Type and Mutant RI Subunits of cAMP-Dependent Protein Kinase[a]

protein	C_m	$\Delta G°_{H_2O}$	m	C_m with 150 μM cAMP	$\Delta G°_{H_2O}$	m
wt-RI	4.8	7.0	−1.3	5.8	9.5	−1.3
stripped wt-R	4.2	3.7	−0.9	6.2	nd	nd
R(M329W)	4.6	6.5	−1.2	5.8	9.0	−0.9
R(R209K)	3.6	3.8	−1.0	3.8	4.0	−1.0
R(R333K)	4.3	4.4	−1.1	3.6, 6.0	nd	nd
Δ(260−379)R	4.8	7.2	−1.3	6.1	9.2	−1.2

[a] The midpoint concentrations (C_m) were all calculated from the data depicted in Figures 6 and 8C. The unfolding was carried out using purified proteins where the cAMP-binding sites were saturated and in the presence of 150 μM excess cAMP. The protein concentration was 0.5 μM R dimer. Standard error values were 0.1−0.2 M for C_m, 0.04−0.2 kcal/mol for $\Delta G°_{H_2O}$, and 0.01−0.02 kcal mol^{-1} M^{-1} for m.

Table 2: Iodide Quenching of Tryptophan Fluorescence of RI Subunits[a]

protein	no. of Trp residues	quenching 0 M urea	quenching 3 M urea	quenching 7 M urea
wt-R	3	0.3	0.8	1.0
R(R209K)	3	0.5	0.7	1.0
R(R333K)	3	0.5	0.8	1.0
R(M329W)	4	0.4	0.3	1.0
Δ(260−379)R	2	0.0	1.0	1.0

[a] Iodide quenching of the wild-type RIα subunit, the R(R209K), R(R333K), and R(M329W) point mutants, and the Δ(260−379)R deletion mutant, in the presence of 0, 3, or 7 M urea. Quenching was expressed as the fraction of tryptophan fluorescence susceptible to iodide quenching, as calculated from the modified Stern−Volmer plot. Errors for fractional quenching values were 0.01−0.03 M.

R(M329W) than for wt-R, probably reflecting the susceptibility of Trp329 to quenching. In the presence of 3 M urea, 70% of the fluorescence of R(R209K) and 80% of the fluorescence of R(R333K) were quenched, compared to 80% for wt-R. R(M329W) exhibited a remarkable resistance to quenching, with only 30% of its fluorescence quenched at 3 M urea. Finally, at 7 M urea, all the Trp fluorescence was quenched in every protein.

Characterization of a Deletion Mutant Lacking Domain B and Trp260. Δ(260−379)R was characterized to ascertain the influence of domain B on the stability of domain A. This mutant R subunit binds cAMP to site A, binds the C subunit, and is activated in response to cAMP like the full-length wt-R (*30*). The Trp fluorescence in the absence of urea was slightly shifted to red, indicating that removal of domain B slightly changed the environment of the two remaining tryptophans (Figure 8A, arrow). At the same protein concentration, the mutant's fluorescence intensity was approximately 65% of that observed for wt-R, and close to that of R(W260Y) (*20*). The increase in fluorescence from 0 to 3 M urea was comparable to that of wt-R (Figure 5A), and was 25% higher at 3 M urea than in the absence of urea (Figure 8B). The small shift in λ_{max} between 0 and 4 M urea paralleled that of wt-R (Figure 8B), being much smaller than the shift of R(R333K). After the fluorescence reached a maximum at 4 M urea, the spectra shifted to longer wavelengths.

The unfolding curve for Δ(260−379)R had a C_m of 4.8 M urea (Figure 8C and Table 1), identical to that of wt-R. The addition of l50 μM cAMP shifted the C_m to 6.1 M, with no changes in cooperativity (Figure 8C and Table 1). Therefore, this mutant mostly behaved like wt-R. Deletion of domain B, including Trp260, did not significantly destabilize either. Unlike wt-R and the point mutants, Δ-

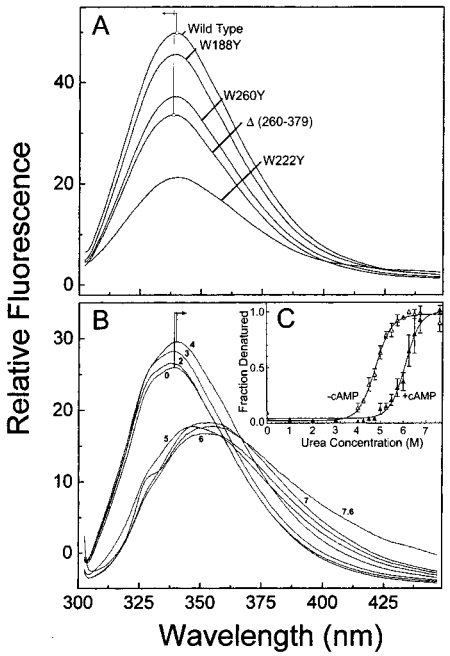

FIGURE 8: Fluorescence characterization of the Δ(260−379)R deletion mutant. (A) Comparison of the fluorescence emission spectrum of Δ(260−379)R with the spectra of wt-R and several Trp mutants. Each protein was saturated with cAMP. The arrow indicates the direction of the change in λ_{max} for Δ(260−379)R compared to wt-R. (B) Trp fluorescence spectra of Δ(260−379) at various urea concentrations. Concentrations are indicated on each spectrum. The arrow indicates the direction of the shift in λ_{max} that accompanies the increase in urea concentration from 0 to 4 M. (C) Unfolding curves for Δ(260−379)R as a function of urea concentration. The R subunit (0.5 μM) was denatured in the absence of excess cAMP (white symbols) or in the presence of 150 μM excess cAMP (black symbols). The protein samples were excited at 293 nm at 23 °C in buffer A.

(260−379)R showed little or no quenching of the Trp fluorescence in the absence of urea (Table 2). Since Trp188 is exposed in wt-R, the lack of quenching at 0 M urea suggests changes in the global structure of Δ(260−379)R that shield Trp188 from the solvent. All the fluorescence of Δ(260−379)R was quenched at 3 M urea, strongly suggesting that the structural changes induced by the deletion of domain B facilitated the access of iodide to Trp222.

DISCUSSION

Understanding how the cooperative binding of cAMP to the two cAMP-binding sites of the regulatory subunit of cAPK promotes dissociation of the C subunit is fundamental for comprehending this "on/off" switch at a molecular level. Thus, we evaluated the structural stability of recombinant R subunits that contained one defective cAMP-binding site. Previously, we characterized the unfolding of the wt-R subunit (*19*) and the role of each tryptophan residue (*20*) using fluorescence spectroscopy and CD. Those studies, together with the crystal structural of RIα (*18*), were invaluable to interpret the observations reported in the work presented here. Our experimental system contains three Trp residues: Trp188, Trp222, and Trp260. Trp260 and Trp222 are in buried locations and contribute 25 and 65%, respectively, to the total fluorescence emission of wt-R (*20*) (Figure 8A). Trp188 is positioned on an exposed loop in domain A (Figure 1A), and its contribution to the fluorescence of wt-R is only 10% (*20*) (Figure 8A).

Each cAMP-binding site mutant used in this study had a single-point mutation that replaced a conserved Arg in the cAMP-binding site with Lys. Kinetic analysis of cAMP binding showed that the mutation of either site abolished high-affinity cAMP binding to that site, and simultaneously lowered the cAMP-binding affinity of the adjacent site (*29*). Replacing Arg209 with Lys in R(R209K) decreased K_d(cAMP) approximately 1 order of magnitude (*41*). Also, direct binding studies proved that R(R333K) binds cAMP to site A with high affinity, although there is a slight increase in K_d (*29*). As a result, the purified mutant proteins did not have cAMP bound to the defective domain. In contrast, in wt-R both cAMP-binding sites remained saturated with cAMP following purification (*28*).

The fluorescence intensity of R(R209K) was higher than that of wt-R, and λ_{max} was shifted to higher wavelengths. This could be explained by the lack of quenching of Trp260 fluorescence by cAMP, and possibly by changes in the environment of Trp222. Conversely, there was a decrease in the emission intensity of R(R333K), without any change in λ_{max}. Although in R(R333K) domain A functions normally, the fluorescence emission of the tryptophans in domain A is perturbed, suggesting long-range interdomain interactions.

CD measurements showed a correlation between disruption of cAMP binding and global changes in secondary structure for R(R209K), but not for R(R333K). This was concordant with analytical gel filtration data which indicated that R(R333K) and wt-R had the same Stokes radius (43 ± 0.5 Å), whereas the radius of R(R209K) was reduced to 41.5 ± 0.6 Å (*29*). R(R209K) was less stable in the presence of urea, as shown by fluorescence and CD. There was a decrease in the cooperativity of the unfolding and C_m, and unlike the wt-R, excess cAMP had no stabilizing effect. However, this reduction in C_m and the loss of cooperativity were smaller than for R(R209K).

One interesting feature of R(R333K) was the biphasic unfolding in the presence of excess cAMP. The biphasic profile most likely reflected the separate unfolding of the two domains. The first component could reflect the unfolding of the mutated domain B at low urea concentrations. As in wt-R, the intact site A could be stabilized by excess cAMP. Accordingly, the second component may reflect the unfolding of domain A at higher urea concentrations.

Quenching of R(R209K) in the absence of urea indicated that the tryptophans were more exposed to the solvent than in wt-R. Quenching of R(R333K) was nearly identical, suggesting that the loss of cAMP in domain B caused conformational changes in domain A.

Our results prove that Arg209 is a critical structural component. Arg209, like Arg333, interacts directly with cAMP, but its modification has a more profound effect on the overall structural stability of the R subunit. The different response of domain A versus domain B may be attributed to the location of the Trp residues closer to site A, yet the CD results in the presence of urea, as well as complementary observations from the literature (*23*, *24*, *29*, *42*), correlate well with the our Trp fluorescence data. To learn more about the stability of domain B and to introduce a probe in domain B, the R(M329W) mutant was engineered. Homology modeling using the crystal structure of wt-R as a template, followed by energy minimization with Trp (data not shown), suggests that Trp329 is mostly exposed to the solvent and

in proximity to α-helix C. The increase in the fluorescence of R(M329W) with respect to wt-R (15%) is comparable to the contribution of Trp188 to the overall fluorescence emission of wt-R (10%), and therefore consistent with the positioning of Trp329 in a similarly exposed location.

Although this mutant had an extra Trp in domain B, the unfolding curve in the absence of excess cAMP was virtually identical to that of wt-R. Unlike wt-R, excess cAMP reduced the cooperativity of the unfolding of R(M329W). Since domain B modulates the cooperative binding of cAMP to site A, the loss of cooperativity may be caused by changes in domain B, which could result in a partial uncoupling of both domains. Cooperativity in cAMP binding is also lost when Tyr371, which interacts with Arg333 (Figure 1C), is replaced with a Phe (*41*). The region extending from Gly323 to Ala335 is linked by an extensive network of contacts that are synergistically dependent on the presence of cAMP (Figure 1C) (*18*). Trp329 is located on α-helix B′, in proximity to α-helix C. The communication between domains A and B is carried out through helix C to the interdomain hydrophobic region, and then transmitted to site A through residues Asp267, Arg241, Glu200, and Trp260 (*18*), which directly interacts with cAMP. Consequently, the destabilization introduced by Trp329 may perturb the interaction of Trp260 with cAMP in domain A and uncouple both domains. A W260Y mutant (*20*) behaved like R(M329W). In the absence of excess cAMP, there were no differences between wt-R and the mutant. In the presence of excess cAMP, there was a decrease in cooperativity. Again, this suggested that in R(M329W) the perturbation was transmitted from the vicinity of binding site B to Trp260 via helix C.

Another atypical feature of R(M329W) was the reduced Trp solvent accessibility at low urea concentrations. Since Trp188 and, possibly, Trp329 are exposed, it is reasonable to assign the increased level of quenching at 0 M urea to those residues, and the unusual behavior at 3 M urea to residues Trp260 and/or Trp222. Trp260 may be quenched less efficiently by cAMP when the protein is partially unfolded by low urea concentrations, which would account for the increased emission and reduced quenching.

Δ(260−379)R, which lacks domain B, provided further insights into the intrinsic stability of domain A and the influence of the adjacent domain. Since the deletion mutant forms stable complexes with the C subunit, domain B is not essential for the R−C interaction (*30*). Trp260 is in direct contact with cAMP. Interestingly, removal of domain B, including Trp260, or replacement of Trp260 with Tyr (*20*) had no effect on unfolding. Therefore, although Trp260 plays a key role in interdomain communication, it is not crucial for the structural stability of domain A.

In the presence of urea, Δ(260−379)R and wt-R had comparable stabilities. The stability of Δ(260−379) as a function of NaCl concentration or pH is also comparable to that of wt-R (*43*). The R209K mutation was far more destabilizing for domain A than the deletion of domain B. The R333K mutation also had a greater effect on stability than the deletion of the whole domain, confirming the influence of interdomain communication on the structural stability of domain A. The domain deletion influenced the conformation of domain A, based on several lines of evidence. wt-R is affinity labeled by 8-N_3-cAMP at Trp260 (*46*). However, in Δ(260−379)R, a new site located in the α-helix C:A (Figure 1A), Tyr244, was labeled (*4*). Labeling of Tyr244, which in wt-R is far from the cAMP-binding pocket, requires a rearrangement that moves the C helix closer to the cAMP-binding site of the deletion mutant. The absence of Trp260 and Arg241, which keep the helix away from the barrel in wt-R (*18*), makes this possible. When domain B is absent, helix C probably collapses onto the β-barrel, adopting a conformation that may shield Trp188 from the solvent, as suggested by the lack of quenching in the absence of urea.

Δ(260−379)R is more susceptible to quenching at 3 M urea than any of the other mutants studied and wt-R. In wt-R, the mobility of helix C is restricted by hydrophobic interactions with domain B and by the interaction of Trp260 with the cAMP bound to site A. In Δ(260−379)R, the absence of those restrictions would be enough to expose both Trp residues at 3 M urea.

These findings, together with the mutation of other residues critical for cAMP binding and interdomain communication, provide the foundation for an improved understanding of the interactions between the R monomers, and between them and the catalytic subunit.

ACKNOWLEDGMENT

We thank Anna Canaves for her assistance in manuscript preparation and graphics design and Angel Yap for the molecular models in Figure 1.

REFERENCES

1. Taylor, S. S., Buechler, J. A., and Yonemoto, W. (1990) *Annu. Rev. Biochem. 59*, 971.
2. Dell'Acqua, M. L., and Scott, J. D. (1997) *J. Biol. Chem. 272*, 12881.
3. Fantozzi, D. A., Harootunian, A. T., Wen, W., Taylor, S. S., Feramisco, J. R., Tsien, R. Y., and Meinkoth, J. L. (1994) *J. Biol. Chem. 269*, 2676.
4. Ringheim, G. E., Saraswat, L. D., Bubis, J., and Taylor, S. S. (1988) *J. Biol. Chem. 263*, 18247.
5. Bubis, J., Vedvick, T. S., and Taylor, S. S. (1987) *J. Biol. Chem. 262*, 14961.
6. Rannels, S. R., Cobb, C. E., Landiss, L. R., and Corbin, J. D. (1985) *J. Biol. Chem. 260*, 3423.
7. Reimann, E. M. (1986) *Biochemistry 25*, 119.
8. Weber, W., and Hilz, H. (1979) *Biochem. Biophys. Res. Commun. 90*, 1074.
9. Leon, D. A., Herberg, F. W., Banky, P., and Taylor, S. S. (1997) *J. Biol. Chem. 272*, 28431.
10. Carr, D. W., Stofko-Hahn, R. E., Fraser, I. D., Bishop, S. M., Acott, T. S., Brennan, R. G., and Scott, J. D. (1991) *J. Biol. Chem. 266*, 14188.
11. Scott, J. D., Stofko, R. E., McDonald, J. R., Comer, J. D., Vitalis, E. A., and Mangili, J. A. (1990) *J. Biol. Chem. 265*, 21561.
12. Herberg, F. W., Dostmann, W. R. G., Zorn, M., Davis, S. J., and Taylor, S. S. (1994) *Biochemistry 33*, 7485.
13. Takio, K., Smith, S. B., Krebs, E. G., Walsh, K. A., and Titani, K. (1982) *Proc. Natl. Acad. Sci. U.S.A. 79*, 2544.
14. Titani, K., Shoji, S., Ericsson, L. H., Walsh, K. A., Neurath, H., Fisher, E. H., Takio, K., Smith, S. B., Krebs, E. G., and Demaille, J. G. (1981) *Cold Spring Harbor Conf. Cell Proliferation 8*, 19.
15. Døskeland, S. O., and Øgreid, D. (1984) *J. Biol. Chem. 259*, 2291.
16. Robinson-Steiner, A. M., and Corbin, J. D. (1983) *J. Biol. Chem. 258*, 1032.
17. Weber, I. T., Steitz, T. A., Bubis, J., and Taylor, S. S. (1987) *Biochemistry 26*, 343.

18. Su, Y., Dostmann, W. R., Herberg, F. W., Durick, K., Xuong, N. H., Ten Eyck, L., Taylor, S. S., and Varughese, K. I. (1995) *Science 269*, 807.
19. Leon, D. A., Dostmann, W. R. G., and Taylor, S. S. (1991) *Biochemistry 30*, 3035.
20. Leon, D. A., Canaves, J. M., and Taylor, S. S. (2000) *Biochemistry 39*, 5662.
21. Øgreid, D., and Døskeland, S. O. (1981) *FEBS Lett. 129*, 282.
22. Øgreid, D., and Døskeland, S. O. (1981) *FEBS Lett. 129*, 287.
23. Gibson, R. M., Buechler, Y.-J., and Taylor, S. S. (1997) *J. Biol. Chem. 272*, 16343.
24. Gibson, R. M., and Taylor, S. S. (1997) *J. Biol. Chem. 272*, 31998.
25. Durgerian, S., and Taylor, S. S. (1989) *J. Biol. Chem. 264*, 9807.
26. Saraswat, L. D., Filutowics, M., and Taylor, S. S. (1986) *J. Biol. Chem. 261*, 11091.
27. Sanger, F., Nicklen, S., and Coulson, A. R. (1977) *Proc. Natl. Acad. Sci. U.S.A. 74*, 5463.
28. Bubis, J., Neitzel, J. J., Saraswat, L. D., and Taylor, S. S. (1988) *J. Biol. Chem. 263*, 9668.
29. Herberg, F. W., Taylor, S. S., and Dostmann, W. R. G. (1996) *Biochemistry 35*, 2934.
30. Saraswat, L. D., Ringheim, G. E., Bubis, J., and Taylor, S. S. (1988) *J. Biol. Chem. 263*, 18241.
31. Buechler, Y. J., Herberg, F. W., and Taylor, S. S. (1993) *J. Biol. Chem. 268*, 16495.
32. Bohm, G., Muhr, R., and Jaenicke, R. (1992) *Protein Eng. 5*, 191.
33. Sreerama, N., and Woody, R. W. (1994) *J. Mol. Biol. 242*, 497.
34. Compton, L. A., and Johnson, W. C., Jr. (1986) *Anal. Biochem. 155*, 155.
35. Manavalan, P., and Johnson, W. C., Jr. (1987) *Anal. Biochem. 167*, 76.
36. Deléage, G., and Geourjon, C. (1993) *Comput. Appl. Biosci. 9*, 197.
37. Andrade, M. A., Chacón, P., Merelo, J. J., and Morán, F. (1993) *Protein Eng. 6*, 383.
38. Pace, C. N. (1986) *Methods Enzymol. 131*, 266.
39. Lehrer, S. S., and Leavis, P. C. (1978) *Methods Enzymol. 49*, 222.
40. Lehrer, S. S. (1971) *Biochemistry 10*, 3254.
41. Bubis, J., Saraswat, L. D., and Taylor, S. S. (1988) *Biochemistry 27*, 1570.
42. Neitzel, J. J., Dostmann, W. R. G., and Taylor, S. S. (1991) *Biochemistry 30*, 733.
43. Ringheim, G. E., and Taylor, S. S. (1990) *J. Biol. Chem. 265*, 4800.
44. Adler, A., Greenfield, N. J., and Fasman, G. D. (1973) *Methods Enzymol. 27*, 675.
45. Chen, Y. H., Yang, J. T., and Chau, K. H. (1974) *Biochemistry 13*, 3350.
46. Bubis, J., and Taylor, S. S. (1987) *Biochemistry 26*, 3478.

BI001563Q